Iğdır Üniversitesi Fen Bilimleri Enstitüsü Dergisi, 11(3): 1948-1958, 2021
Journal of the Institute of Science and Technology, 11(3): 1948-1958, 2021

ISSN: 2146-0574, eISSN: 2536-4618

Fizik / Physics **DOI: 10.21597/jist.849054**

Araştırma Makalesi / *Research Article*

Geliş tarihi / Received: 29.12.2020 **Kabul tarihi / Accepted: 08.03.2021**

To Cite: Kilic ME, 2021. The Diffusion and Clustering Formation of Gold Atoms on Alpha-Graphyne. Journal of the Institute of Science and Technology, 11(3): 1948-1958.

The Diffusion and Clustering Formation of Gold Atoms on Alpha-Graphyne

Mehmet Emin KILIC[1*]

ABSTRACT: Motivated by the experiment, high mobility of gold atoms on two-dimensional carbon sheets, we examine the ground-state structures, mobility, and clustering formations of small gold clusters (Au_n, n = 1-4) on monolayer alpha-graphyne using first-principles DFT calculations and finite temperature MD simulations. We reveal that Au_n cluster prefers to locate at the center of a hexagon in alpha-graphyne. The binding energy of Au_n on alpha-graphyne increases with increasing the number (n) of gold atoms. Moreover, we predict the step-wise formation of Au_2 out of two pre-adsorbed Au_1 ad-atoms. Likewise, the formation of Au_3 and Au_4 is also considered in the same way. The diffusion energy barrier of Au_1 on alpha-graphyne is found to be only 0.26 eV, indicating the high mobility of gold atoms on alpha-graphyne. Remarkably, the energy required for the cluster formation of gold atoms on alpha-graphyne is about less than 0.2 eV. According to our MD simulations at room temperature (RT), the Au_n cluster is subsequently formed on alpha-graphyne. Considering the high mobility of a single gold atom, the strong binding energy of small gold clusters, and the easy clustering of Au_n at RT on alpha-graphyne, we suggest that alpha-graphyne is a suitable substrate for gold cluster formation.

Keywords: Clustering formation, diffusion, gold adsorption, graphyne, two-dimensional materials

[1]Mehmet Emin KILIC (**Orcid ID:** 0000-0003-1814-5104), Korea Institute of Science and Technology, Computational Science Center, Seoul, Republic of Korea

***Sorumlu Yazar/Corresponding Author:** Mehmet Emin KILIC, e-mail: mekilic@kist.re.kr

INTRODUCTION

The discovery of graphene (Novoselov, 2004) has led to emerge a new era in material science due to its various remarkable mechanical and electronic properties including zero-gap semiconductor nature, ultrahigh carrier mobility, and unusual high intrinsic thermal conductiovity (Novoselov et al., 2005; Zhang et al., 2005; Yan et al., 2008). Since then, the list of 2D materials (graphyne (Baughman et al., 1987), silicene (Okamoto et al., 2010), and many more (Kilic et al., 2016; Ipek et al., 2018; Pekoz et al., 2018; Kilic et al., 2020) is fast expanding.

Carbon is a remarkable facile element because it can form *sp*, sp^2, and/or sp^3 hybridization, resulting in the formation of new carbon-based chemical bonds having quite different properties (Kilic et al., 2020, Kilic et al., 2021). For instance, graphene, constructed with one atomic layer of sp^2-hybridized carbons, is a zero-gap semiconductor or semimetal and soft property whereas diamond consisting of sp^3-hybridized carbons, has an electrical insulating material and excellent hardness (Novoselov et al., 2005; Kaner, 2005).

Graphyne, theoretically proposed in 1987 (Baughman et al., 1987), is mono-atomic-thick planar sheets of *sp*- and sp^2-bonded carbons. Graphdiyne, belongs to the same family as graphyne, has been synthesized via different approaches (Haley et al., 1997; Johnson et al., 2007; Li et al., 2010; Wang et al., 2018). Graphyne was found to be energetically more stable than graphdiyne (Kim et al., 2012), suggesting that many stable phases of graphyne would be synthesized in the near future. The presence of the acetylenic linkage and "natural pores" make graphyne promising one-atom-thickness carbon allotrope that exceptional properties. Such that, some graphyne allotropes (alpha-, beta-, and 6,6,12-graphyne) show Dirac-cone electronic band structures (Kim et al., 2012). Some other graphyne allotropes (gamma-graphyne), on the other hand, present intrinsically non-zero band gap feature, promising for next-generation electronic applications (Kim et al., 2012). Moreover, its unique structure with natural porous and large surface area can be utilized for a variety of potential applications in gas separation (Cranford et al., 2012), water filtration (Kou et al., 2014), energy storage (Guo et al., 2012).

Metal decorated graphyne systems are highly important for energy storage, catalysis, and sensing applications. Alkali metal decorated graphyne was reported to be potential for hydrogen storage applications (Li et al., 2011). Noble metals can improve the sensing properties of graphyne in sensor performance, and proposed a suitable substrate for single atom catalysts with high catalytic activity (Ma et al., 2015; Kong et al., 2017). Gold nanoparticles on carbon-based materials (graphite, graphene, and graphyne) have attracted considerable interest for various applications in nanoelectronics, sensors, energy storage, and so on (Wang et al., 2004; Jensen et al., 2004; Ming et al., 2005; Carara et. al., 2009; Amft et al., 2011). Remarkably, McCreary et al. (McCreary et al., 2010) studied the role of the distribution of gold atoms on the charge carrier mobility of graphene. They revealed that the formation of gold clusters enhances the mobility whereas their homogeneous distribution results in reducing the mobility ratio. With this motivation, attention has recently been focused on small gold nanoparticles on carbon-based systems (Amft et al., 2011; Azizi et al., 2014; Chen et al., 2018).

Herein, we have examined the adsorption of gold clusters (Au_n) on single layer alpha-graphyne, their mobility and clustering formation both using first-principles DFT calculations and finite temperature MD simulations. We have further investigated the stepwise formation mechanism of Au_2 out of two pre-adsorbed Au_1 ad-atoms as well as the formation of Au_3 and Au_4 on the graphyne sheet. The high mobility of Au atoms on alpha-graphyne and the easy clustering formation of Au atoms on the sheet have been revealed.

MATERIALS AND METHODS

Density of Functional Calculations

First-principle calculations were performed using spin-polarized density functional theory (DFT) within the generalized gradient approximation (GGA) in the form of Perdew-Burke-Ernzerhof (PBE) with the van der Waals correction methods of Grimme as implemented the Vienna Ab-initio Simulation Package (VASP) (Kresse et al., 1994; Blochl, 1994; Perdew et al., 1996; Kresse et al., 1999; Grimme, 2016). Since VASP always employs three dimensional (3D) periodic boundary conditions, a vacuum region of about 20 Å was applied along the z-direction to exclude the inter-sheets interactions. All geometric structures were fully relaxed until energy and forces were converged to 1×10^{-5} eV and 0.001 eV/Å, respectively. The Brillouin zone (BZ) was sampled with a 21×21×1 Γ-centered Monkhorst- Pack (MP) special k-point grids (Monkhorst et. al., 1976). A plane-wave basis with a cutoff energy of 520 eV was employed. For the lattice dynamics phonon calculations, the second order harmonic interatomic force constants were calculated using the Phonopy package (Togo et al., 2015). Using a supercell approach (4×4×1 supercell with 2×2×1 k-mesh), the phonon dispersion curves were computed from the force constants. For the diffusion calculations, the climbing-image NEB method (Henkelman et al., 2000) is used to find minimum energy paths (MEP) and transition states (TS). This method enables to find the MEP given the initial and final states (denoted as IS and FS, respectively). We have taken eight images between IS and FS, and interpolated them. The obtained images are connected by springs, then relaxed. The corresponding images are optimized until the maximum force on the atoms is reached less than 0.01 eV $Å^{-1}$. The TS is verified from the MEP including saddle points

The binding energy of the gold atom(s) on alpha-graphyne is calculated the following expression:

$$E_b = (E_{graphyne} + n\,E_{Au} - E_{Au/graphyne}) / n \quad (1)$$

Where $E_{graphyne}$, E_{Au}, and $E_{Au/graphyne}$, and n are the total energies of pristine alpha-graphyne, an isolate Au atom(s), and Au_n adsorbed graphyne system, and the number of added Au atom per simulation cell, respectively.

Molecular Dynamics Calculations

The clustering formation on alpha-graphyne under temperature was simulated using classical MD simulations conducted by LAMMPS code (Plimpton, 1995). The interactions between C-C within Au_n/alpha-graphyne were modeled using the AIREBO potential (Stuart et al., 2000), which takes into account the bonding as well as non-bonding interactions among atoms. Lenard-Jones potentials were considered for Au-C interactions (Luedtke et al., 1999). For Au-Au interactions, the system was performed via Embedded-atom model (EAM) inter-atomic potential (Foiles et al., 1986). All MD simulations were performed under NVT canonical ensemble. We used Nose-Hoover thermostat in order to control the system temperature (Nose, 1984; Nose, 1984; Hoover, 1985). The periodic boundary conditions (PBC) were applied along the in-plane directions (*x* and *y*). Equations of motion was integrated by the velocity Verlet algorithm. The time step (*t*) of the MD simulations was set for 1 fs.

RESULTS AND DISCUSSION

Pristine Alpha-Graphyne

The unit cell of alpha-graphyne as shown in Figure 1 is used as basic model to study the Au clustering formation. As a benchmark, we first study the structure characterization, lattice dynamics, and electronic band structure of pristine alpha-graphyne. Unlike graphene where all the carbon atoms are connected via the sp^2-hybridization bonding, alpha-graphyne composed of two chemically in-equivalent

carbon atoms, namely *sp*-hybridized carbons (labeled as C_1) and sp^2-hybridized carbons (labeled as C_2). alpha-graphyne has two distinct bond lengths of 1.23 Å between two C_1 atoms (*sp*-*sp*) and 1.40 Å between C_1 and C_2 atoms (sp-sp^2). After full relaxation, the optimized lattice constant *a* is found to be 6.97Å (Figure 1 (b)). The obtained lattice parameters agree well with reported values in the literature (Morshedloo et al., 2016).

To further test the dynamic stability of alpha-graphyne, the lattice dynamics phonon calculations have been performed. The phonon frequencies with respect to *k*-points in the Brillouin zone (BZ) are presented in Figure 1(c). One can easy see that all the phonon modes are positive throughout the BZ and the absence of any imaginary frequency confirms the stability of alpha-graphyne. Similar to graphene, there exist three acoustic phonon branches (namely, transverse in-plane TA, longitudinal LA, and out-of-plane ZA). At near Γ-point, the TA and LA acoustic branches exhibit linear features whereas the feature of ZA branch is quadratic dispersion. After verifying the dynamical stability of alpha-graphyne,

We have investigated its electronic properties. The calculated electronic band structure is presented in Figure 1(d). The valence band maximum (VBM) and conduction band minimum (CBM) of alpha-graphyne cross at a single point (K) at Fermi level, which can be characterized by Dirac cone feature.

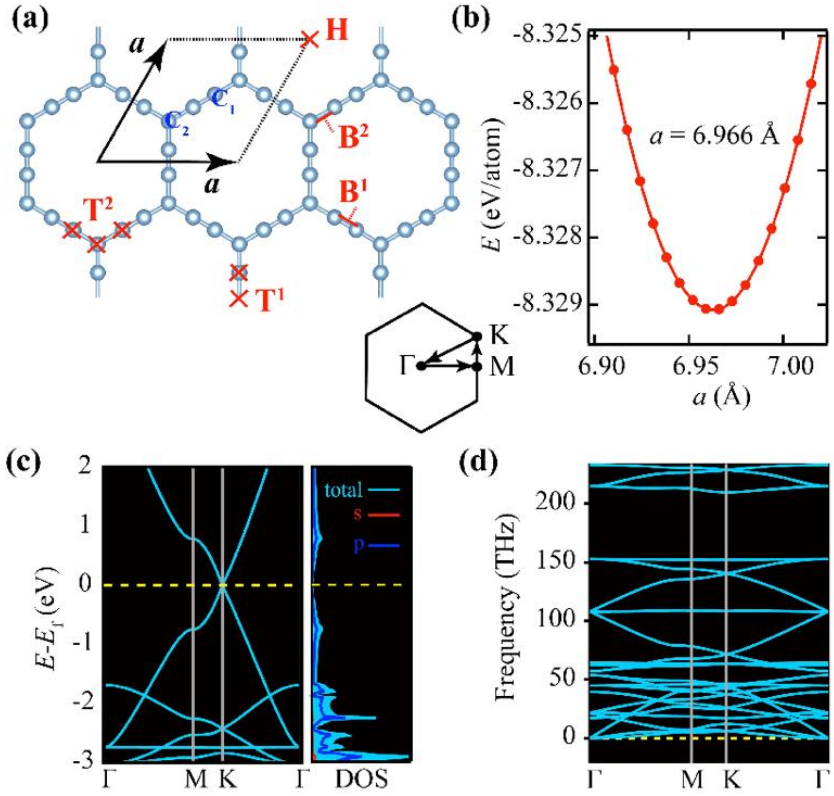

Figure 1. (a) Optimized atomic structure of pristine alpha-graphyne. The unitcell (marked by the black dashed line) is composed of two *sp*- hybridized carbons (denoted as C_1) and six sp^2-hybridized carbons (denoted as C_2). Lattice constant *a* and the considered adsorption sites B^1, B^2, T^1, T^2, and H are depicted in the figure. Blue balls in the lattice indicate C_1 and C_2 atoms. (b) Energy *E* in eV/atom of alpha-graphyne with respect to the lattice a in Å. (c) Electronic band structure at the GGA-PBE functional level and atom-orbital projected density-of-states (DOS). The Fermi level energy (E_f) is set to zero (yellow dashed line). (d) Phonon dispersion curves along with the high symmetric *k* points as from Gamma to M, M to K and K to Gamma (inset).

Au_n Adsorption on Alpha-Graphyne

First, we have investigated the interaction of Au_1 with alpha-graphyne using spin polarized DFT calculations, To determine the energetically favorable position of Au_1 atom on alpha-graphyne, we

have considered five different adsorption sites: top of C_1 and C_2 atoms (denoted as T^1 and T^2, respectively), bridge between two C_1 atoms and between C_1 and C_2 atoms (denoted as B^1 and B^2, respectively), and hollow site (denoted as H) with in-plane and out-of-plane configurations in the 2x2 supercell (Figure 1 (a)). After the energy optimization, we have found that the B^1, B^2 and T^2 sites with both in-plane and out-of-plane configurations are unfavorable for the Au_1 adsorption on alpha-graphyne. The Au_1 atom located at these unfavorable sites with out-of-plane configurations would gradually migrate to T^1 site (out-of-plane) whereas for in-plane configuration would gradually move to H site (in-plane) during the structure relaxation process. Therefore, the T^1 (out-of-plane) and H (in-plane) sites are found to be two energetic sites with 0.93 eV and 0.78 eV binding energies, respectively, to adsorb the Au_1 on alpha-graphyne (see Figure 2 (a)).

To examine the presence of the spin and electronic states, we have analyzed the spin projected density of states (DOS) for the T^1 site (see Figure 3). One can easy see that the spin up and spin down are not axially symmetrical near the Fermi energy, resulting in the magnetic properties. The DOS below Fermi level (namely occupied states) corresponds to the majority of spin-up electrons inducing the spin polarization with 1.0 μ_B magnetic moment. The Au_1 bonded carbon atom (Au bonded C atom just underneath the Au_1 atom change 0.68 Å upward towards to basal plane of the carbon at which the bond bond length $d_{C\text{-}Au}$ is about be 2.04 Å, and generating a small atomic distortion for the second and third neighbors of the Au-bonded C atom. Therefore, the adsorbed Au_1 atom on the T^1 site of alpha-graphyne induces local lattice distortion. This configuration was referred to as Au_1/alpha-graphyne. For H site, on the other hand, the atomic distortions are relatively small, and the magnetic moment is found to be 0 μ_B. Considering the atomic distortions, symmetry, magnetization, and small energy difference in binding energy between the two energetic sites (T^1 and H), the H site to adsorb Au_1 on alpha-graphyne would be more favorable than the T^1 site.

Next, we have studied the adsorption of gold dimer (Au_2) on the sheet. To determine the most energetic position of the Au_2 on the sheet, we consider its all possible combinations. Figure 2(b) shows two energetic configurations of the Au_2 on alpha-graphyne with out-of-plane and in-plane configurations. The calculated binding energy of Au_2 on alpha-graphyne is about 1.22 and 1.93 eV for out-of-plane and in-plane configurations, respectively. Thus, the Au_2 energetically prefers to locate on the center of hexagon of the alpha-graphyne as a lateral position with small out-of-plane configuration with h = 0.78 Å, at which the dimer gold atoms are bounded to the *sp*-hybridized carbons as shown in Figure 2(b), right. This configuration is referred to as Au_2/alpha-graphyne where the d_1 (C-Au) and d_2 (Au-Au) bond lengths are about 2.20 Å and 2.47 Å, respectively. The calculated total magnetic moment for the Au_2/alpha-graphyne is found to be zero.

Likewise, the adsorption of gold trimer (Au_3) on the 2x2 monolayer alpha-graphyne is investigated. After the energy optimization, we have found that the Au_3 is also preferentially located in the hexagon of the alpha-graphyne as a lateral position, and h = 1.30 Å out-of-plane configuration illustrated in Figure 2(c), right. This configuration is referred to as Au_3/alpha-graphyne. The calculated binding energy of the Au_3 on alpha-graphyne system is about 3.04 eV with 1 μ_B total magnetic moment. The d_1 (C-Au) and d_2 (Au-Au) bond lengths found to be 2.24 Å and 2.61 Å, respectively.

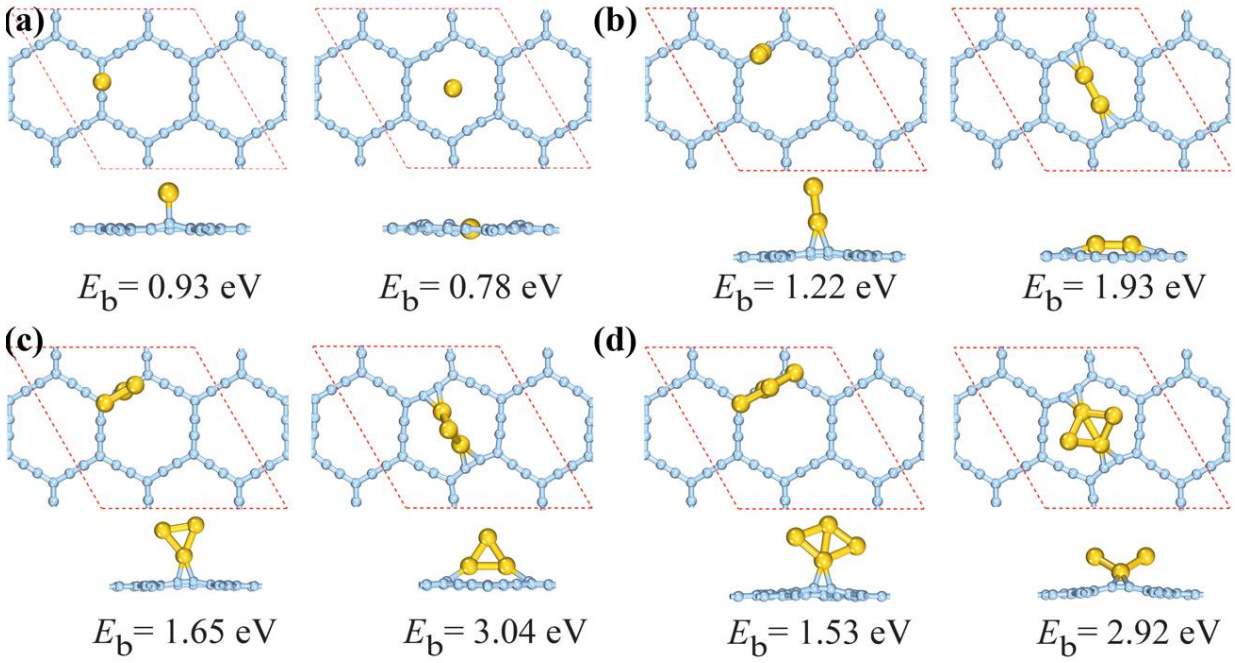

Figure 2. Two energetic atomic configurations of Au_n (n = 1-4) adsorption on 2x2 alpha-graphyne sheet. C and Au atoms are in sky blue and in yellow, respectively.

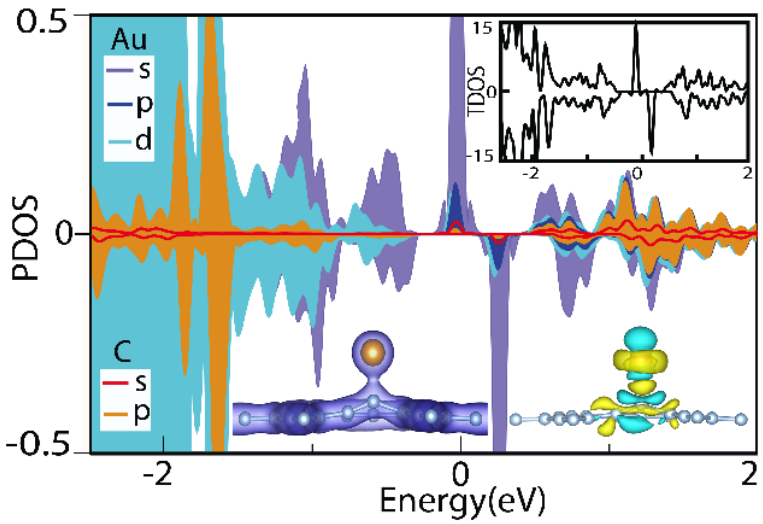

Figure 3. Total and projected density of states (PDOS) of a single Au atom located at the T^1 site of alpha-graphyne, total density of states (TDOS) (inset), and charge density difference where yellow and cyan iso-surface indicate electron accumulation and depletion, respectively (inset).

Finally, we examined the adsorption of gold tetramer (Au_4) on the 2x2 monolayer alpha-graphyne. The most energetic position of Au_4 is given in Figure 2(d) with 2.92 eV binding energy and zero magnetic moments. The adsorbed Au_4 located at the hexagon of alpha-graphyne induces a local distortion of the hexagons due to the size of Au_4. The d_1 (C-Au) and d_2 (Au-Au) bond lengths are found to be 2.76 Å and 2.65 Å, respectively. We note that Au_n/alpha-graphyne (where n is odd number) system exhibits magnetic behavior whereas Au_n/alpha-graphyne (where n is even number) exhibits non-magnetic feature. Comparing the magnetic systems (or non-magnetic systems), the increase the number of Au atoms on alpha-graphyne results in an increase in the binding energy, and thus leading to clustering formation.

The Diffusion and Clustering Formation

We have further evaluated the Au_1 atom diffusion on the alpha-graphyne using NEB calculations. We set the initial diffusion path by considering the energetic sites for the Au_1 atom on alpha-graphyne. The atomic configuration of the initial state (IS), transition state (TS), final state (FS), and the optimized minimum energy path (MEP) for the Au_1 atom diffusion is presented in Figure 4. The activation energy barrier of the Au_1 atom to diffuse from the IS to FS on the alpha-graphyne is found to be 0.26 eV. This low energy barrier indicates the high mobility of Au_1 atom diffusion from one energetic site (T^1) to another on alpha-graphyne. We also note that the B^1 site between the IS and FS of the MEP are found to be TS.

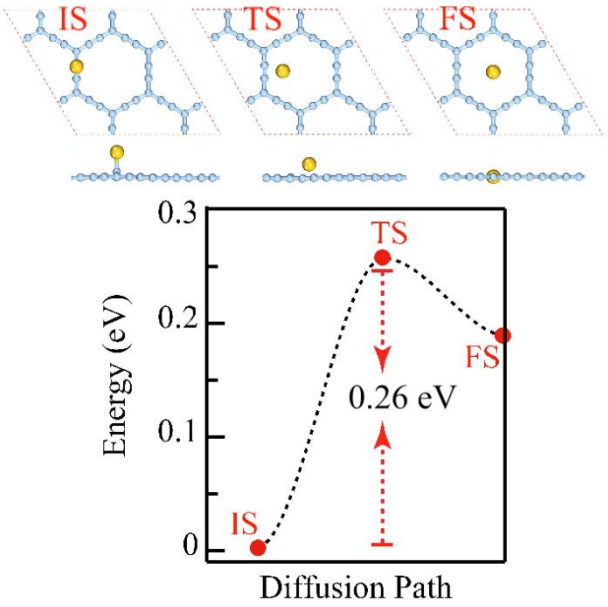

Figure 4. Calculated MEP for a single Au atom on the alpha-graphyne. The optimized atomic arragements of IS, TS, and FS are depicted. The IS and FS are first and second energeticics sites for the single Au atom adsorption on alpha-graphyne.

As initial step for the clustering formation, we have further studied the formation of a dimer (Au_2) on the sheet. To examine the energy barrier for the formation of Au_2 on the sheet, two pre-adsorbed Au_1 atom is initially placed at the two different T^1 sites (which is ground state position of the single Au atom adsorption). Figure 5 shows the atomic positions of the IS, TS, and FS and the optimized MEP for the Au_2 formation on alpha-graphyne. The energy barrier for the considered reaction path is about 0.12 eV, which is lower than that of the Au_1 atom on the alpha-graphyne sheet. This promotes easy cluster formation. We further studied the formation a trimer (Au_3) on alpha-graphyne. We accomplish the formation of the Au_3 by allowing pre-adsorbed Au_1 and Au_2 (Au_1 and Au_2 $\rightarrow$ Au_3) to full relax from the initial energetic positions. Similarly, the formation of Au_4 out of a trimer and ad-atom (Au_1 and Au_2 $\rightarrow$ Au_3) was taken placed at the center of hexagon without encountering any energy barriers.

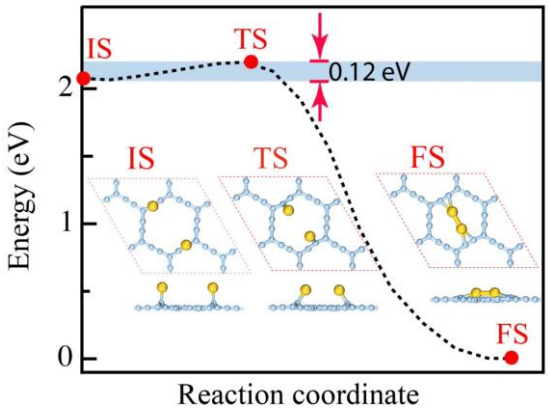

Figure 5. MEP for a gold dimer Au_2 on the alpha-graphyne. The optimized atomic configurations of the IS, TS, and FS are depicted.

Finally, we studied the Au cluster formation on alpha-graphyne under temperature via performing molecular dynamics (MD) simulation, which is a powerful tool and enable us to simulate large systems with long time scale. Our constructed 2D system (alpha-graphyne) was composed an 80x48x1 supercell with a cell length of 56.8 nm and 59.08 nm along the *x* and *y* lattice directions, respectively, and contains 61440 C atoms with periodic boundary conditions (along the *x* and *y* directions). To examine the Au_n clustering formation on the constructed graphyne, 7680 Au atoms were initially placed at T^1 sites with out-of-plane configuration. We observed that the Au atoms were subsequently clustered in the center of hexagons of the alpha-graphyne with different Au ratio even at 300 K temperature. Most importantly, when the Au atoms were initially located at the H sites of alpha-graphyne with in-plane configuration (see Figure 6, upper panel), the Au clusters were formed under temperature (T = 300 K) as presented in Figure 6, lower panel.

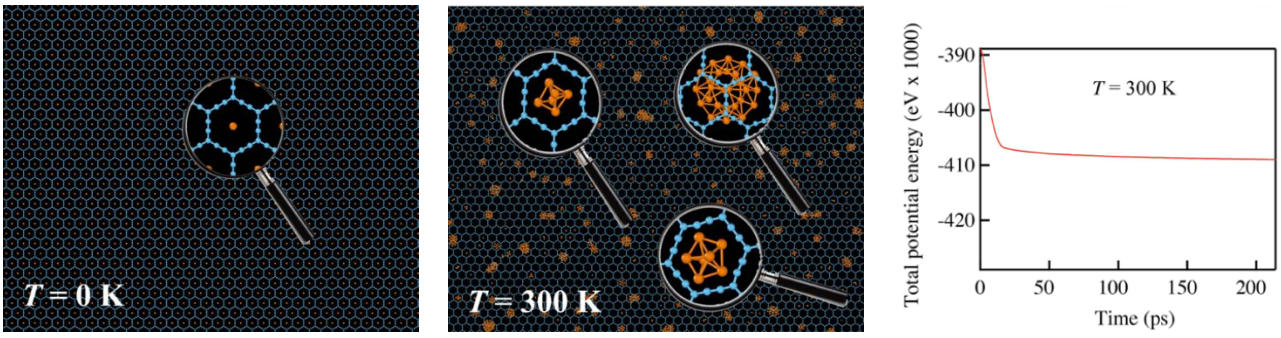

Figure 6. Atomic configuration of Au_1/alpha-graphyne system (where all the Au atoms located at the center of hexagon in alpha-graphyne) at T = 0 K upper panel and T = 300 K middle panel. Lower panel represents the total energy as a function of time (in ps) at T = 300 K**.**

CONCLUSION

Using first-principles DFT calculations and finite temperature MD simulations, we have examined the energetically favorable positions of small gold clusters (Au_n) on monolayer alpha-graphyne, their mobility and clustering formation. We have realized that the Au_n prefers to locate at the center of hexagon in alpha-graphyne. The Au_n/alpha-graphyne (where n is odd number) system exhibits magnetic behavior whereas Au_n/alpha-graphyne (where n is even number) exhibits non-magnetic feature. The calculated binding energy for the Au_n on alpha-graphyne increases with increasing the number (n) of gold atoms. The step-wise formation of Au_2 out of two pre-adsorbed Au_1 as well as the formation of Au_3 and Au_4 are examined. The diffusion energy barrier of a single gold adatom Au

on alpha-graphyne is only 0.26 eV, indicating the high mobility of Au atom on alpha-graphyne. The energy requiring for the cluster formation of gold atoms is less than 0.2 eV. Based on the MD simulations, the Au clusters were subsequently formed under thermal shock even at room temperature (RT). Considering the high mobility of Au atom, strong binding energy of small gold clusters, and the easy clustering of Au_n at RT, alpha-graphyne is a suitable substrate for gold cluster formation.

ACKNOWLEDGEMENTS

This work was supported by the Brain Pool Program through the National Research Foundation of Korea (NRF) funded by the Ministry of Science and ICT (2020H1D3A1A02081517).

Author's Contributions

Mehmet Emin Kilic: Conceptualization, Investigation, Writing, Reviewing Visualization and Supervision.

Conflict of Interest

The article authors declare that there is no conflict of interest between them.

REFERENCES

Amft M, Sanyal B, Eriksson O, Skorodumova NV, 2011. Small Gold Clusters on Graphene, their Mobility and Clustering: a DFT Study. Journal of Physics: Condensed Matter, 23: 205301.

Azizi E, Tehrani ZA, Jamshidi Z, Interactions of Small Gold Clusters, Aun (n=1–3), with Graphyne: Theoretical Investigation, 2014. Journal of Molecular Graphics and Modelling, 54: 80.

Baughman RH, Eckhardt H, Kertesz M, 1987. Structure-Property Predictions for New Planar Forms of Carbon: Layered Phases Containing s p 2 and s p Atoms. The Journal of Chemical Physics, 87: 6687.

Blochl PE, 1994. Projector Augmented-Wave Method. Physical Review B, 50: 17953.

Carara SS, Batista RJC, Chacham H, 2009. Modifications in Graphene Electron States Due to a Deposited Lattice of Au Nanoparticles: Density Functional Calculations. Physical Review B, 80: 115435.

Chen D, Tang J, Zhang X, Cui H, Li Y, 2018. Sulfur Dioxide Adsorbed on Pristine and Au Dimer Decorated γ-Graphyne: A Density Functional Theory Study, Applied Surface Science, 458: 781.

Cranford SW, Buehler MJ, 2012. Selective Hydrogen Purification Through Graphdiyne under Ambient Temperature and Pressure. Nanoscale, 4: 4587.

Foiles SM, Baskes MI, Daw MS, 1986. Embedded-Atom-Method Functions for the Fcc Metals Cu, Ag, Au, Ni, Pd, Pt, and their Alloys. Physical Review B, 33: 7983.

Grimme S, 2006. Semiempirical GGA-Type Density Functional Constructed with a Long-Range Dispersion Correction. Journal of Computational Chemistry, 27: 1787.

Guo Y, Jiang K, Xu B, Xia Y, Yin J, Liu Z, 2012. Remarkable Hydrogen Storage Capacity in Li-Decorated Graphyne: Theoretical Predication, The Journal of Physical Chemistry C, 116: 13837.

Haley MM, Brand SC, Pak JJ, 1997. Carbon Networks Based on Dehydrobenzoannulenes: Synthesis of Graphdiyne Substructures. Angewandte Chemie International Edition, 36: 836.

Henkelman G, Uberuaga BP, Jonsson HA, 2000. Climbing Image Nudged Elastic Band Method for Finding Saddle Points and Minimum Energy Paths. The Journal of Chemical Physics, 113: 9901.

Hoover WG, 1985. Canonical Dynamics: Equilibrium Phase-Space Distributions. Physical Review A, 31: 1695.

Ipek S, Kilic ME, Mogulkoc A, Cahangirov S, Durgun E, 2018. Semiconducting Defect-Free Polymorph of Borophene: Peierls Distortion in Two-Dimensions. Physical Review B, 98: 241408.

Jensen P, Blase X, Ordejon P, 2004. First-Principles Study of Gold Adsorption and Diffusion on Graphite. Surfice Science, 564: 173.

Johnson CA, Lu Y, Haley MM, 2007. Carbon Networks Based on Benzocyclynes. 6. Synthesis of Graphyne Substructures via Directed Alkyne Metathesis. Organic Letters, 9: 3725.

Kilic ME, Erkoc S, 2016. Structural Properties of Pristine and Defected ZnO Nanosheets under Biaxial Strain: Molecular Dynamics Simulations. Journal of Nanoscience and Nanotechnology, 16: 1506.

Kilic ME, Lee K-R, 2020. Tuning the Electronic, Mechanical, Thermal, and Optical Properties of Tetrahexcarbon via Hydrogenation, Carbon, 161: 71.

Kilic ME, Lee K-R, 2020. First-principles Study of Fluorinated Tetrahexcarbon: Stable Configurations, Thermal, Mechanical, and Electronic Properties, The Journal of Physical Chemistry C, 124: 8225

Kilic ME, Lee K-R, 2021. Tetrahex Carbides: Two-dimensional Group-IV Materials for Nanoelectronics and Photocatalytic Water Splitting, Carbon, 174: 368.

Kaner RB, 2005. Material Science: Designing Superhard Materials. Science, 308: 1268.

Kim BG, Choi HJ, 2012. Graphyne: Hexagonal Network of Carbon with Versatile Dirac Cones. Physical Review B, 86: 115435.

Kresse G, Hafner J, 1994. Norm-Conserving and Ultrasoft Pseudopotentials for First-Row and Transition Elements, Journal of Physics: Condensed Matter, 6: 8245.

Kresse G, Joubert D, 1999. From Ultrasoft Pseudopotentials to the Projector Augmented-Wave Method. Physical Review B, 59: 1758.

Kong X, Huang Y, Liu Q, 2017. Two-Dimensional Boron-Doped Graphyne Nanosheet: A New Metal-Free Catalyst for Oxygen Evolution Reaction. Carbon, 123: 558.

Kou J, Zhou X, Lu H, Wu F, Fan J, 2014. Graphyne as the Membrane for Water Desalination, Nanoscale, 6: 1865.

Li C, Li J, Wu F, Li S-S, Xia J-B, Wang L-W, 2011. High Capacity Hydrogen Storage in Ca Decorated Graphyne: a First-Principles Study. The Journal of Physical Chemistry C, 115: 23221.

Li G, Li Y, Liu H, Guo Y, Li Y, Zhu D, 2010. Architecture of Graphdiyne Nanoscale Films. Chemical Communications, 46: 3256.

Luedtke WD, Landman U, 1999. Slip Diffusion and Lévy Flights of an Adsorbed Gold Nanocluster. Physical Review Letter, 82: 3835.

Ma DW, Li T, Wang Q, Yang G, He C, Ma B, Lu Z, 2015. Graphyne As a Promising Substrate for the Noble-Metal Single-Atom Catalysts. Carbon, 95: 756.

McCreary KM, Pi K, Swartz AG, Han W, Bao W, Lau CN, Guinea F, Katsnelson MI, Kawakami RK, 2010. Effect of Cluster Formation on Graphene Mobility. Physical Review B, 81: 115453.

Monkhorst HJ, Pack JD, 1976. Special Points for Brillouin-Zone Integrations. Physical Review B, 13: 5188.

Morshedloo T, Roknabadi MR, Behdani M, Modarresi M, Kazempour A, 2016. First Principle Study of Inducing Superconductivity in α-Graphyne by Hole-Doping and Biaxial Tensile Strain. Computational Material Science, 124: 183.

Nose S, 1984. A Unified Formulation of the Constant Temperature Molecular Dynamics Methods. The Journal of Chemical Physics, 81: 511.

Nose S, 1984, A Molecular Dynamics Method for Simulations in the Canonical Ensemble. Molecular Physics, 52: 255.

Novoselov KS, 2004. Electric Field Effect in Atomically Thin Carbon Films. Science, 306: 666.

Novoselov KS, Geim AK, Morozov S, Jiang D, Katsnelson MI, Grigorieva IV, Dubonos SV, Firsov AA, 2005. Two-Dimensional Gas of Massless Dirac Fermions in Graphene. Nature, 438: 197.

Okamoto H, Kumai Y, Sugiyama Y, Mitsuoka T, Nakanishi K, Ohta T, Nozaki H, Yamaguchi S, Shirai S, Nakano H, 2010. Silicon Nanosheets and their Self-Assembled Regular Stacking Structure. Journal of the American Chemical Society, 132: 2710.

Pekoz R, Konuk M, Kilic ME, Durgun E, 2018. Two-Dimensional Fluorinated Boron Sheets: Mechanical, Electronic, and Thermal Properties. ACS Omega, 3: 1815.

Perdew JP, Burke K, Ernzerhof M, 1996. Generalized Gradient Approximation Made Simple, Physical Review Letter, 77: 3865.

Plimpton S, 1995. Fast Parallel Algorithms for Short-Range Molecular Dynamics. Journal of Computational Physics, 117: 1.

Stuart SJ, Tutein AB, Harrison JA, 2000. A Reactive Potential for Hydrocarbons with Intermolecular Interactions. The Journal of Chemical Physics., 112: 6472.

Togo A, Chaput L, Tanaka I, 2015. Distributions of Phonon Lifetimes in Brillouin Zones. Physical Review B, 91, 094306.

Wang GM, BelBruno JJ, Kenny SD, Smith R, 2004. Gold Adatoms and Dimers on Relaxed Graphite Surfaces. Physical Review B, 69: 195412.

Wang GM, BelBruno JJ, Kenny SD, Smith R, 2005. Density Functional Study of Aun (n=3–5) Clusters on Relaxed Graphite Surfaces. Surface Science, 576: 107.

Wang T, Huang J, Lv H, Fan Q, Feng L, Tao Z, Ju H, Wu X, Tait SL, Zhu J, 2018. Kinetic Strategies for the Formation of Graphyne Nanowires via Sonogashira Coupling on Ag (111). Journal of the American Chemical Society, 140: 13421.

Yan J-A, Ruan WY, Chou MY, 2008. Phonon Dispersions and Vibrational Properties of Monolayer, Bilayer, and Trilayer Graphene: Density-Functional Perturbation Theory. Physical Review B, 77: 125401.

Zhang Y, Tan Y-W, Stormer HL, Kim P, 2005. Experimental Observation of the Quantum Hall Effect and Berry's Phase in Graphene. Nature, 438: 201.